Boletim da Sociedade Astronômica Brasileira, **35**, no. 1, 16-17

Determination of the interstellar medium components towards the molecular cloud CO225.30-66.30

A. Carli[1], W. Corradi[2,1], N. Sasaki[3,2], & W. Reis[4,1]

[1] UFMG e-mail: antoniobfc@ufmg.br
[2] LNA e-mail: wbcorradi@lna.br
[3] UEA e-mail: nsasaki@uea.edu.br
[4] IBMEC e-mail: wilsonr@fisica.ufmg.br

Abstract. In this work we have analysed the sctructure of the interstellar medium in the direction of the molecular cloud CO225.30-66.30, using data of absorption in the visible and distance obtained from the Starhorse catalog (Anders et al. (2022)). Through the analysis of color excess vs. distance diagrams and maps of the spatial distribution of the reddening, we have identified three components along the line of sight. The first transition occurs at (400 ± 25) pc in the western part of the cloud, identified to be the shell of the Orion-Eridanus Superbubble. A second transition occurs at (600 ± 25) pc in the eastern part of the cloud, possibly the back of the Superbubble, and a third transition, identified as the cloud itself, that shows up at (750 ± 40) pc. In the future we intend to use polarimetric data, collected at Observatório do Pico dos Dias - OPD/LNA, to refine these results.

Resumo. Neste trabalho analisamos a estrutura do meio interestelar na direção da nuvem molecular CO225.30-66.30, utilizando valores de absorção no visível e de distância obtidas do catálogo Starhorse (Anders et al. (2022)). Através da análise de diagramas de excesso de cor por distância, e também de mapas de distribuição espacial do avermelhamento, identificamos três componentes ao longo da linha de visada. A primeira transição ocorre em (400 ± 25) pc, na área mais à oeste da nuvem, envoltório da Superbolha Órion-Eridanus. Uma segunda transição ocorre em (600 ± 25) pc, possivelmente a parte de trás da Superbolha, na parte mais a leste da nuvem, e uma terceira transição, identificada como a nuvem, ocorre em (750 ± 40) pc. No futuro usar dados polarimétricos coletados no Observatório do Pico dos Dias - OPD/LNA, para refinar esses resultados..

Keywords. ISM: clouds – dust, extinction, distance

1. Introduction

This paper is part of a broader study of the physical properties of the interstellar medium , particularly of the molecular clouds and the young stellar objects associated with them, in order to understand interstellar bubbles and their distribution on the local interstellar medium, i.e. up to 2 kpc of the Sun (Santos et al. (2011) e Reis et al. (2011)).

Several cold clouds have been identified by the Planck Satellite, one of them being the molecular cloud CO225.30-66.30, previously observed by Keto et al. (1986), in the Galactic coordinates (225.24, -66.29). This cloud stands low and far from the Galactic Disc, being close to the Orion-Eridanus Superbubble (OE-S) shell.

CO225.30-66.30, shown on Fig. 1, appears to be a single structure, but with a strange shape on its top part, which may be two different structures in the same line of sight, or be caused by the magnetic field, creating a shape resembling a fish's head.

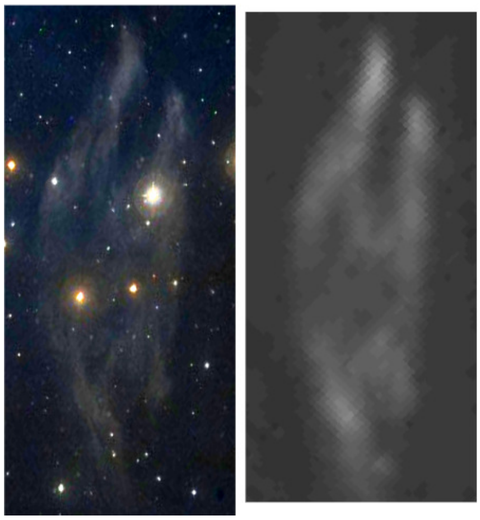
]

Figure 1. The cloud CO225.30-66.30 on visible DSS (left) and on IRAS 100 μm(right).

2. Methodology

In order to analyse our data, we have made color excess E(b-y) vs. distance (kpc) diagrams and maps of the reddening spatial distribution, identifying components of the interstellar medium along the line of sight, following the method of Corradi et al. (1997, 2004) and Reis & Corradi (2008).

The idea is to identify transitions in color excess E(b-y) vs. distance (kpc) diagrams, where a sudden increase in the color excess arises towards the cloud, when compared to regions out of the cloud's line of sight. So the distance to the cloud can be determined. The determination of the uncertainties were obtained for each star individually.

For our data, we have used the distance and absorption in the visible Av, taken from the Starhorse catalog (Anders et al. (2022)), which utilizes Gaia EDR3 data, to determine the reddening $E(b-y) = Av/4.3$.

We have chosen to extract the data in a circular area with a radius of 30 arcmin centered in the coordinates (Ra, Dec): (39,71°; -29,59°), shown in Fig. 2. The initial sample resulted in 575 stars. Our confidence interval goes from 0 to 2% in the distance and 0.009 *mag* in the reddening, and our selection criteria was the percentile P05 and P95 for distance and color excess, eliminating stars with an error greater than 15% in both cases. The final sample resulted in 94 targets.

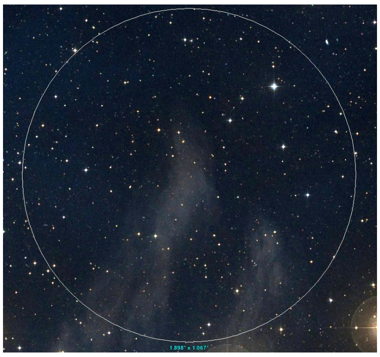

Figure 2. Circular area of 30 arcmin radius centered in the coordinates (Ra, Dec): (39,71°; -29,59°) encompassing the CO225.30-66.30 cloud.

3. Results

On Fig. 3 we can see our final sample with a color scheme indicating the color excess of the stars, going from light blue (-0.01 mag) to black (0.20 mag).

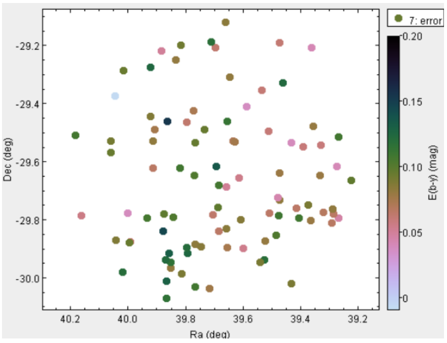

Figure 3. Reddening Spatial Map for our final sample. A color scheme for the color excess is indicated in the colorbar; from light blue (-0.01 mag) to black (0.20 mag).

We have separated our sample in four parts, those being the western part of the cloud (blue), the eastern part of the cloud (green), outside the cloud (gray) and a transition region (pink), which can be seen on Fig. 4.

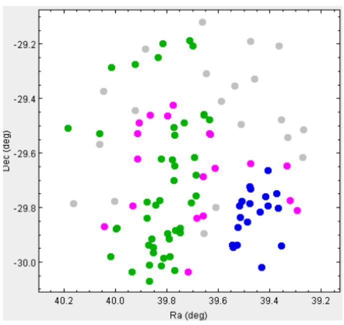

Figure 4. Reddening Spatial Map with the sample separated in four parts: western part of the cloud (blue), the eastern part of the cloud (green), outside the cloud (gray) and a transition region (pink).

The color excess vs. distance diagram is shown in Fig. 5. We have identified three transitions: in the eastern cloud (green) at (400 ± 25) pc, indicated by the green arrow; in the western cloud (blue) at (600 ± 25) pc, indicated by the blue arrow and in the whole cloud at (750 ± 40) pc, indicated by the red arrow.

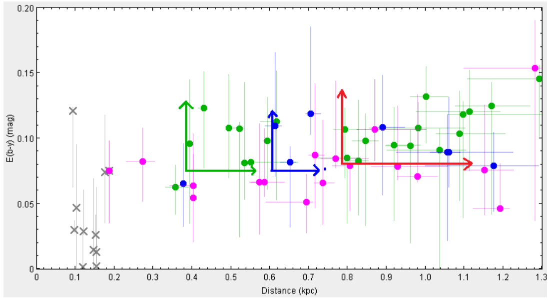

Figure 5. Colour Excess E(b-y) vs. Distance Diagram for our final sample with error bars. The western part of the cloud is shown in blue, the eastern part in green and the transition region in pink. Data with high errors are shown in gray crosses. We identified three sudden increases in the color excess: the first at (400 ± 25) pc, the second at (600 ± 25) pc and the third, which indicates the cloud's distance, at (750 ± 40) pc, shown by the arrows.

The transition at (400 ± 25) pc indicates a thin layer of dust that can be associated with the outer shell of the Orion-Eridanus Superbubble, which occurs at this distance, as observed by Reis et al. (2011), while the transition at 600 pc can't be as well defined because of the lack of data between 400 and 600 pc. It may be possibly identified with the back of the Superbubble. The transition at (750 ± 40) pc indicates the distance of the cloud, since the whole amount suffers an increase in the reddening to a minimum of 0,08 mag.

4. Conclusions

Our analysis of the interstellar medium components in the direction of the molecular cloud CO225.30-66.30 suggest three transitions along the line of sight to the cloud.

The first transition occurs at (400 ± 25) pc, indicating a thin layer of dust that can be associated with the Orion-Eridanus Superbubble. The second transition, at (600 ± 25) pc can also be caused by the OE-S, since the lack of data between 400 and (600 ± 25) pc makes it harder to identify the proper position. The distance to the cloud is suggested to be (750 ± 40) pc, where we observed an increase in the mininum reddening of the stars throughout the whole region, with a large spread of the reddening values right in this distance.

In the future, we intend to use polarimetric data collected with the IAGPOL at the Observatório do Pico dos Dias - OPD/LNA to refine these results. The degree of polarization and the polarization angle of the stars in the line of sight to the cloud may allow us to understand the origin of the cloud's fish head shape.

Acknowledgements. The authors wish to acnkowledge the support from UFMG, LNA and UEA, the Gaia Collaboration as well as the Topcat developers.

References

Anders F. et al. (2022), A&A 658, A91
Corradi W. J. B. et al. (1997), A&A, 326, 1215
Corradi W. J. B. et al. (2004), A&A, 347, 4
Keto E.R. et al. (1986), ApJ 304, 466
Reis, W. et al. (2011), ApJ 734, 8
Santos, F.P. et al. (2011), ApJ 728, 104